

# Tissue Processing of Nitrite in Hypoxia

## AN INTRICATE INTERPLAY OF NITRIC OXIDE-GENERATING AND -SCAVENGING SYSTEMS<sup>\*(§)</sup>

Received for publication, August 27, 2008, and in revised form, September 23, 2008. Published, JBC Papers in Press, October 3, 2008, DOI 10.1074/jbc.M806654200

Martin Feelisch<sup>†§1</sup>, Bernadette O. Fernandez<sup>‡§2</sup>, Nathan S. Bryan<sup>‡2</sup>, Maria Francisca Garcia-Saura<sup>‡</sup>, Selena Bauer<sup>‡</sup>, David R. Whitlock<sup>||</sup>, Peter C. Ford<sup>\*\*</sup>, David R. Janero<sup>†††</sup>, Juan Rodriguez<sup>§§</sup>, and Houman Ashrafian<sup>¶¶</sup>

From the <sup>†</sup>Whitaker Cardiovascular Institute, Boston University School of Medicine, Boston, Massachusetts 02118, the <sup>§</sup>Clinical Sciences Research Institute, University of Warwick, Warwick Medical School, Coventry CV4 7AL, United Kingdom, the <sup>¶</sup>Brown Foundation Institute of Molecular Medicine, University of Texas-Houston Health Science Center, Houston, Texas 77030, <sup>||</sup>Nitroceutic LLC, Dover, Massachusetts 02030, the <sup>\*\*</sup>Department of Chemistry and Biochemistry, University of California, Santa Barbara, California 93106, the <sup>††</sup>Center for Drug Discovery, Northeastern University, Boston, Massachusetts 02115, the <sup>§§</sup>Department of Physics, Centenary College of Louisiana, Shreveport, Louisiana 71134, and the <sup>¶¶</sup>Department of Cardiovascular Medicine, University of Oxford, Oxford OX3 9DU, United Kingdom

Although nitrite ( $\text{NO}_2^-$ ) and nitrate ( $\text{NO}_3^-$ ) have been considered traditionally inert byproducts of nitric oxide (NO) metabolism, recent studies indicate that  $\text{NO}_2^-$  represents an important source of NO for processes ranging from angiogenesis through hypoxic vasodilation to ischemic organ protection. Despite intense investigation, the mechanisms through which  $\text{NO}_2^-$  exerts its physiological/pharmacological effects remain incompletely understood. We sought to systematically investigate the fate of  $\text{NO}_2^-$  in hypoxia from cellular uptake *in vitro* to tissue utilization *in vivo* using the Wistar rat as a mammalian model. We find that most tissues (except erythrocytes) produce free NO at rates that are maximal under hypoxia and that correlate robustly with each tissue's capacity for mitochondrial oxygen consumption. By comparing the kinetics of NO release before and after ferricyanide addition in tissue homogenates to mathematical models of  $\text{NO}_2^-$  reduction/NO scavenging, we show that the amount of nitrosylated products formed greatly exceeds what can be accounted for by NO trapping. This difference suggests that such products are formed directly from  $\text{NO}_2^-$ , without passing through the intermediacy of free NO. Inhibitor and subcellular fractionation studies indicate that  $\text{NO}_2^-$  reductase activity involves multiple redundant enzymatic systems (*i.e.* heme, iron-sulfur cluster, and molybdenum-based reductases) distributed throughout different cellular compartments and acting in concert to elicit NO signaling. These observations hint at conserved roles for the  $\text{NO}_2^-$ -NO pool in cellular processes such as oxygen-sensing and oxygen-dependent modulation of intermediary metabolism.

Nitric oxide ( $\text{NO}$ )<sup>3</sup> is the archetypal effector of redox-regulated signal transduction throughout phylogeny, from microorganisms to plants and animals (1). The conserved influences of NO extend from the regulation of basic cellular processes such as intermediary metabolism (2), cellular proliferation (3), and apoptosis (4) to systemic processes such as hypoxic vasoregulation (5). Mammalian NO production has been attributed to the enzymatic activity of NO synthases, nitrate ( $\text{NO}_3^-$ )/nitrite ( $\text{NO}_2^-$ ) reductases and non-enzymatic  $\text{NO}_2^-$  reduction (6). The NO produced is believed to act directly as a signaling molecule by binding to the heme of soluble guanylyl cyclase or nitrosating peptide/protein cysteine residues (7). More recently, it has become apparent that  $\text{NO}_2^-$ , previously considered an inert byproduct of NO metabolism present in plasma (50–500 nM) and tissues (0.5–25  $\mu\text{M}$ ), is, under some conditions, also a source of NO/nitrosothiol signaling (6, 8). Although the importance of  $\text{NO}_2^-$  has received increasing appreciation (9) as being central to processes including exercise (10), hypoxic vasodilation (11), myocardial preconditioning (12, 13), and angiogenesis (14), controversy surrounds the chemistry, kinetics, and tissue specificity of  $\text{NO}_2^-$  bioactivity (15, 16). Perhaps the greatest uncertainty pertains to the role of heme moieties in  $\text{NO}_2^-$  metabolism (6, 10, 12, 13, 15–22). We therefore sought to address systematically the path of  $\text{NO}_2^-$  biotransformation in hypoxic tissues and its processing into NO and NO-related species across levels of biological organization by employing an experimental paradigm that ranges from cellular  $\text{NO}_2^-$  uptake *in vitro* to tissue  $\text{NO}_2^-$  utilization *in vivo*. Our findings reveal that multiple heme, iron-sulfur cluster, and molybdenum-based reductases, distributed among distinct subcellular compartments, act in a cooperative manner to convert  $\text{NO}_2^-$  to NO and related signaling products. The correlation between  $\text{NO}_2^-$  reductase activity and oxidative phosphorylation capacity across organs suggests that  $\text{NO}_2^-$  serves a cell regulatory role (*e.g.* the modulation of intermediary metabolism) beyond its capacity to elicit hypoxic vasodilatation.

\* This work was supported, in whole or in part, by National Institutes of Health Grants HL 69029 (to M. F.) and the Kirschstein National Research Service Award Cardiovascular Training Grant (to B. O. F. and N. S. B.). This work was also supported by the Medical Research Council (MRC Strategic Appointment Scheme, to M. F.), and a Wellcome Trust CVRI Fellowship (to H. A.). The costs of publication of this article were defrayed in part by the payment of page charges. This article must therefore be hereby marked "advertisement" in accordance with 18 U.S.C. Section 1734 solely to indicate this fact.

§ The on-line version of this article (available at <http://www.jbc.org>) contains supplemental information, Table S1, and Figs. S1 and S2.

<sup>1</sup> To whom correspondence should be addressed: Clinical Sciences Research Institute, University of Warwick, Warwick Medical School, Gibbet Hill Road, Coventry, CV4 7AL, UK. Tel.: 44-0-2476-528372; Fax: 44-0-2476-150589; E-mail: mf@warwick.ac.uk.

<sup>2</sup> Both authors contributed equally to this work.

<sup>3</sup> The abbreviations used are: NO, nitric oxide; ALDH2 (mtALDH2), mitochondrial aldehyde dehydrogenase 2; DPI, diphenyleioidonium; EthOx, ethoxyresorufin; Hb, hemoglobin; i.p., intraperitoneal; NaNO<sub>2</sub>, sodium nitrite; NO<sub>2</sub><sup>-</sup>, nitrite; NO<sub>3</sub><sup>-</sup>, nitrate; RBC, red blood cells; RNNO, N-nitrosamines; R5NO, S-nitrosothiols; SNO-Hb, S-nitrosohemoglobin; XOR, xanthine oxidoreductase; PBS, phosphate-buffered saline.

## Nitrite Processing by Hypoxic Tissues

### EXPERIMENTAL PROCEDURES

#### Animals and Reagents

Male Wistar rats (250–350 g) from Harlan (Indianapolis, IN) were allowed food (2018 rodent diet, Harlan) and water *ad libitum* and were maintained on a regular 12 h light/12 h dark cycle with at least 10 days of local vivarium acclimatization prior to experimental use. All protocols were approved by the Institutional Animal Care and Use Committee of the Boston University School of Medicine. All gasses and chemicals were of the highest available grade (see supplemental information for details).

#### Biological Sample Harvest and Preparation

Heparinized (0.07 units/g body weight, intraperitoneal) rats were anesthetized with diethylether and euthanized by cervical dislocation. Whole blood (3–5 ml) was collected from the inferior vena cava into EDTA-containing tubes (1.8 mg/mL) and processed as detailed (23, 24) to obtain RBC and plasma. Isolated, packed RBC (1 blood vol-equivalent) were immediately lysed hypotonically with 3 vol of water. After thoracotomy, a catheter was inserted into the infrarenal portion of the abdominal aorta, and organs were flushed free of blood by retrograde *in situ* perfusion at a rate of 10 ml/min with air-equilibrated PBS before extirpation.  $\text{NO}_2^-$  reductase activity was assessed by measuring the NO generated immediately after addition of 100  $\mu\text{l}$  of a 20 mM  $\text{NaNO}_2$  stock solution to tissue samples (200  $\mu\text{M}$  final  $[\text{NO}_2^-]$ ) using gas-phase chemiluminescence.

#### Liver Homogenate Preparation

Hepatic tissue was acquired by standard techniques (see supplemental information). Liver homogenate was diluted 180-fold in LHM and preincubated at 37 °C for 4 min with either PBS (vehicle control) or a variety of inhibitors (supplemental Table S1) in a light-protected reaction vessel continuously purged with nitrogen. For analysis of inhibitor effects, the amount of NO generated within the first 4 min of incubation in the presence of test compound was compared with a parallel sample treated only with the respective inhibitor vehicle.

#### Nitrite Reductase Activity in Subcellular Fractions

Hepatic subcellular fractions were obtained by differential centrifugation (25). Low-speed centrifugation ( $1,000 \times g$ , 10 min) of whole-liver homogenate (S0) was used to remove undisrupted tissue, nuclei, and particulate debris into the resulting pellet (P1), which was discarded. The supernatant (S1) was recovered and re-centrifuged ( $10,000 \times g$ , 10 min) to obtain a mitochondrial fraction (P2). The corresponding supernatant (S2) was subjected to a final centrifugation ( $105,000 \times g$ , 60 min) to obtain microsomal (P3) and cytosolic (S3) fractions. For analysis of  $\text{NO}_2^-$  reductase activity across fractions, each mitochondrial (P2) and microsomal (P3) pellet was re-suspended in LHM to the same dilution as that of the supernatant fractions from which they were derived and analyzed as described above. The contribution of each subcellular fraction with respect to total hepatic  $\text{NO}_2^-$  reductase activity was calculated by accounting for the individual fractional product yield (6.2% for P2; 1.3% for P3; 77.8% for S3, with 14.7%

discarded as P1 debris). The influence of NAD(P)H (100  $\mu\text{M}$ ) on the conversion of  $\text{NO}_2^-$  to NO by the subcellular fractions was determined as the relative  $\text{NO}_2^-$  reductase activity in the absence or presence of pyridine nucleotide and expressed as percent of control (with no exogenous pyridine nucleotide added).  $\text{NO}_2^-$  interaction with microsomal cytochrome P<sub>450</sub> was assessed by difference spectrophotometry and chemiluminescence (see supplemental information).

#### In Vitro Studies

**$\text{NO}_2^-$  Uptake by RBCs and Tissues**—Rats were anesthetized with diethylether, and 5 ml of arterial blood was collected via cardiac puncture. Blood was immediately centrifuged at  $1,400 \times g$  (8 min, 4 °C). The supernatant was discarded, and the RBC pellet was placed on ice. Blood-free heart and liver tissue was obtained as described above and also kept on ice until use. Tissue (0.5 g) was minced into 2-mm pieces and placed into 2 ml of air-saturated or “hypoxic” (15 min bubbling with air or argon, respectively) PBS and incubated at 37 °C. Following addition of 10  $\mu\text{M}$   $\text{NaNO}_2$ , aliquots of 50  $\mu\text{l}$  were removed after 1, 3, 5, and 10 min and centrifuged briefly (60 s at  $16,100 \times g$ ) to clarify samples prior to  $\text{NO}_2^-/\text{NO}_3^-$  analysis. For uptake measurements by RBC, 4 ml of PBS were added to 1 ml of packed RBC pellet and processed as above. No changes in the concentrations of  $\text{NO}_2^-/\text{NO}_3^-$  were observed in the absence of cells/tissue.

**Tissue Homogenization and Incubation**—Blood-free tissue samples were homogenized in chilled PBS (1:5 w/v) using a Polytron (PT10–35) homogenizer. Just prior to use, samples were brought with PBS to a 6-fold final dilution (v/v) for tissues and a 4-fold final dilution (v/v, equivalent to 2.5% hematocrit) for lysed RBC. For incubation, an equivalent tissue/RBC sample volume was placed into the light-protected reaction vessel of an ozone-chemiluminescence NO analyzer (CLD 77sp, EcoPhysics). The vessel was maintained at 37 °C, and samples were purged sequentially with either medical-grade air (normoxia) or nitrogen (hypoxia/near-anoxia). NO generation was continuously monitored for 5 min following addition of 200  $\mu\text{M}$   $\text{NaNO}_2$  (final conc.). This  $\text{NO}_2^-$  concentration has been established as sufficient to support vasorelaxation *in vitro*, regional vasodilation *in vivo*, and nitrosylation and S-nitrosation of Hb *in vitro* and *in vivo* (10). Aliquots of samples were collected for protein determination, and all values were normalized to total protein.

#### In Vivo Studies

Rats were administered 1.0 mg/kg  $\text{NaNO}_2$ , intraperitoneal. This dosing regimen ensures that  $\text{NO}_2^-$  equilibrates rapidly across all major organ systems, RBC, and plasma to reach a global steady-state prior to tissue sampling (8). Three min after  $\text{NO}_2^-$  injection acute systemic hypoxia was induced by cervical dislocation and maintained for 2 min. Normoxic controls were examined in parallel without subjecting animals to global hypoxia. In both cases, animals were sacrificed 5 min after  $\text{NO}_2^-$  administration. The same *in situ* retrograde perfusion technique was performed as for the *in vitro* studies above except that the perfusate was air-equilibrated PBS supplemented with NEM/EDTA (10 mM/2.5 mM) to eliminate interference by

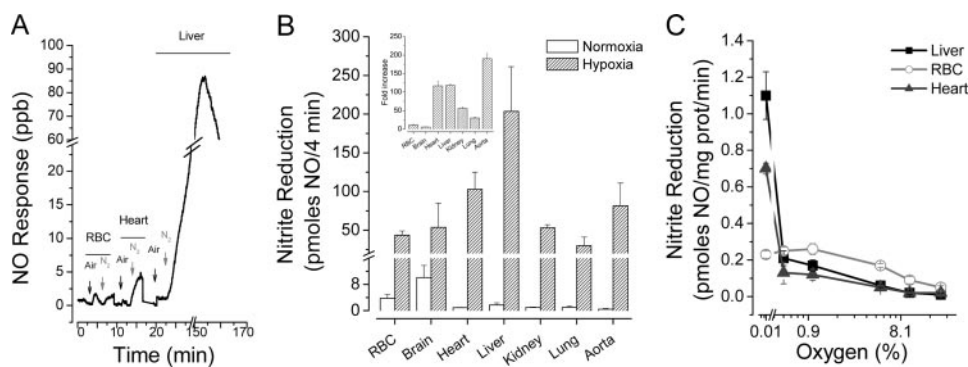


FIGURE 1. Oxygen dependence of  $\text{NO}_2^-$  reduction to NO by different tissues *in vitro*. A, original tracing from blood and tissues under normoxic (Air; 21%  $\text{O}_2$ ) and near-anoxic ( $\text{N}_2$  containing  $\sim 0.01\%$   $\text{O}_2$ ) conditions. B, quantification of NO production (over 4 min) by RBC and different tissues from  $\text{NO}_2^-$  (200  $\mu\text{M}$ ) under normoxic and near-anoxic conditions. C, oxygen-dependence of  $\text{NO}_2^-$  reduction to NO ( $n = 3-4$  per cell/tissue compartment).

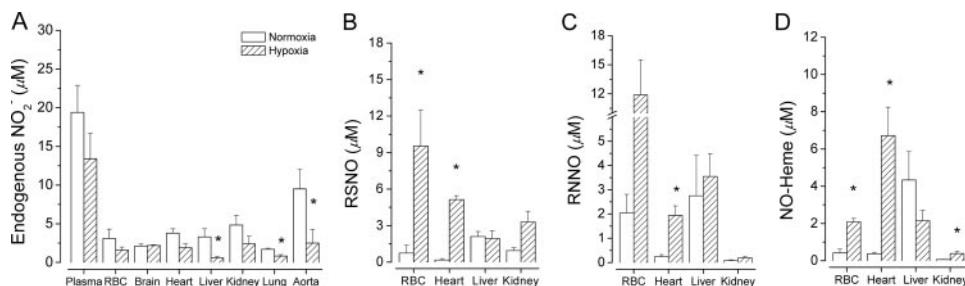


FIGURE 2. Increased formation of tissue NO metabolites from  $\text{NO}_2^-$  during acute global hypoxia *in vivo*. Blood and tissues utilize  $\text{NO}_2^-$  during global hypoxia *in vivo* (A) to generate NO-related products including S-nitrosothiols (RSNO) (B), N-nitrosamines (RNNNO) (C), and iron nitrosyls (NO-heme) (D). ( $n = 3$ ); \*,  $p < 0.05$  versus normoxia.

exogenous  $\text{NO}_2^-$ . NO-related metabolites following  $\text{NO}_2^-$  administration were profiled using previously validated methods (23, 24). NO metabolites include S-nitrosothiols (RSNO), N-nitrosamines (RNNNO), and iron-nitrosyls (NO-heme). Quantification of these species employed group-specific derivatization, denitrosation, and gas-phase chemiluminescence.  $\text{NO}_2^-$  and  $\text{NO}_3^-$  were quantified by ion chromatography (ENO-20, Eicom).

### Data Analysis, Presentation, and Modeling

Unless otherwise noted, data are averages  $\pm$  range from  $n = 3$  individual experiments or means  $\pm$  S.E. from  $n \geq 3$ , as specified. Where appropriate, statistical analysis was performed by one-way analysis of variance with the Bonferroni *post-hoc* test. Least-squares regression analysis was used to characterize the slope and goodness-of-fit of model linear associations between data sets. Spearman rank correlation was applied to evaluate data co-variation. Statistical significance was set at  $p < 0.05$ . Origin 7.0 and Graph Pad Prism 4.0 were used for the statistical analyses. Modeling data were obtained through numeric integration using Mathematica, with a working precision of 20 digits.

## RESULTS

**Tissues Readily Take Up  $\text{NO}_2^-$  in an Oxygen-independent Manner**— $\text{NO}_2^-$  uptake by RBCs, heart, and liver tissue was assessed under normoxic and hypoxic conditions by measuring its disappearance from an external medium containing 10  $\mu\text{M}$   $\text{NO}_2^-$ . Because  $\text{NO}_2^-$  concentrations in these tissues are  $\ll 10$

$\mu\text{M}$  (8, 23, 24), the initial disappearance of  $\text{NO}_2^-$  from PBS should reflect the flux of this anion into the cells/tissues. Indeed,  $\text{NO}_2^-$  is taken up at similar rates by RBC and heart tissue (0.31  $\mu\text{M}/\text{min}$  and 0.24  $\mu\text{M}/\text{min}$ , respectively), and rates are roughly comparable under hypoxic conditions (heart: 0.16  $\mu\text{M}/\text{min}$ ; RBC: 0.28  $\mu\text{M}/\text{min}$ ; see supplemental Fig. S1). Similar data were obtained with liver (not shown). No  $\text{NO}_3^-$  accumulation was seen in the extracellular medium.

**Hypoxia Markedly Potentiates Tissue NO Production from  $\text{NO}_2^-$  in Vitro**—Under aerobic conditions, NO production by RBC and blood-free tissues was minimal even in the presence of 200  $\mu\text{M}$   $\text{NO}_2^-$  (Fig. 1A). Hypoxia/near-anoxia (achieved by  $\text{N}_2$  purging) dramatically enhanced NO formation from  $\text{NO}_2^-$ , particularly by heart, liver, and vascular tissue. NO production by RBC lysate peaked after  $\sim 3$  min, whereas NO production by liver homogenate increased to reach maximal levels after 50–60 min of hypoxia following a brief lag. Near-anoxic,  $\text{NO}_2^-$ -

dependent NO production (standardized as mg protein/min) in all tissues surpassed that of RBC (Fig. 1B). The 2-fold increase in RBC  $\text{NO}_2^-$  reduction from normoxic to near-anoxic conditions is consistent with data previously reported (10). No NO formation was observed when 200  $\mu\text{M}$   $\text{NO}_2^-$  was substituted for  $\text{NO}_3^-$  (not shown).

**NO Generation from  $\text{NO}_2^-$  Is Profoundly Oxygen-dependent**—The oxygen-dependence of tissue  $\text{NO}_2^-$  reductase activity was investigated by adding 200  $\mu\text{M}$   $\text{NaNO}_2$  to liver and heart homogenates and RBC lysate incubated at various oxygen concentrations (21, 10, 5, 1, 0.5, and 0%) and monitoring of the resulting NO formation (Fig. 1C). NO production from  $\text{NO}_2^-$  was maximal under anoxia. Oxygen proved to be a potent inhibitor of  $\text{NO}_2^-$  reduction in liver and heart with  $>80\%$  inhibition at 0.5% oxygen. Less pronounced changes in oxygen dependence were observed with RBC lysate, with maximal rates of NO formation occurring at  $\sim 1\%$  oxygen.

**Acute Hypoxia Potentiates  $\text{NO}_2^-$ -dependent NO Metabolite Formation in Vivo**—To extend the above observations to a more physiological context and to expand on existing observations that hypoxia reduces endogenous brain  $\text{NO}_2^-$  stores coincident with RSNO formation (23), the *in vivo* impact of  $\text{NO}_2^-$  on NO-related metabolite formation was assessed. To ensure initial  $\text{NO}_2^-$  equilibration across all compartments studied, we followed our previous protocol (8) and administered to rats a single intraperitoneal bolus of 1.0 mg/kg  $\text{NaNO}_2$  3 min prior to inducing 2 min of global hypoxia. Acute global hypoxia attenuated  $\text{NO}_2^-$  concentrations in heart, liver, kidney, lung, and aorta (Fig. 2A) and enhanced NO



## Nitrite Processing by Hypoxic Tissues

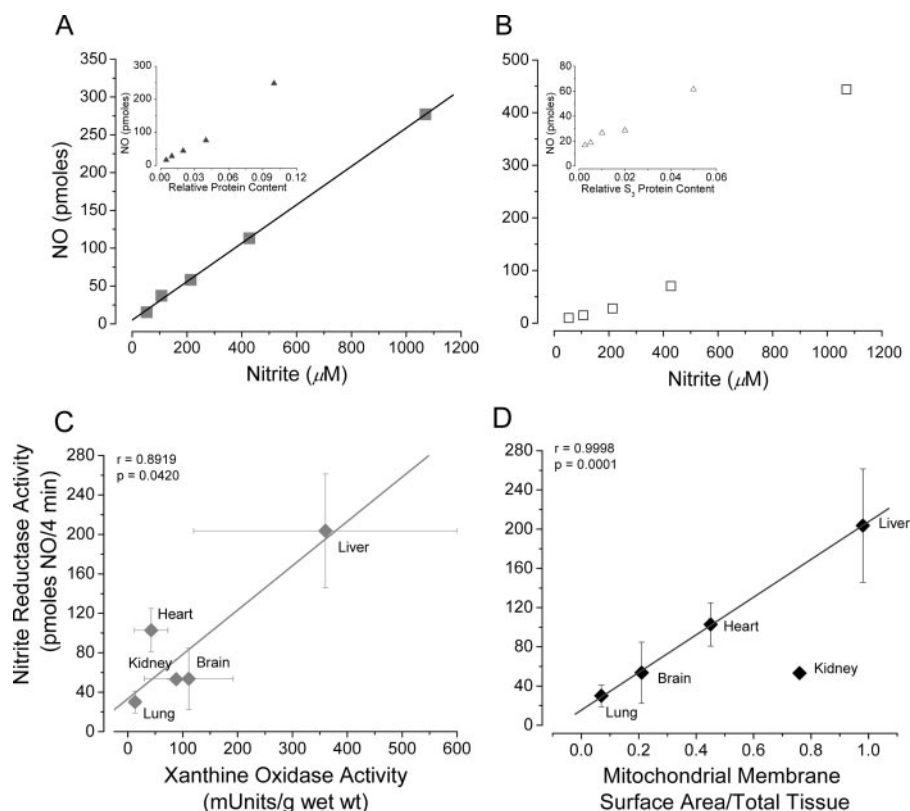


**FIGURE 3. Correlation between NO formation from  $\text{NO}_2^-$  in different tissues and putative  $\text{NO}_2^-$  reductase activity.** A, apparent linear dependence of  $\text{NO}_2^-$  to NO conversion by hypoxic whole liver homogenate (25–1000  $\mu\text{M}$   $\text{NO}_2^-$ ). Inset, hypoxic NO production from 200  $\mu\text{M}$   $\text{NO}_2^-$  is not as linearly dependent upon hepatic protein. B,  $\text{NO}_2^-$  and protein dependence deviate from linearity with the cytosolic fraction. C, significant correlation exists between hypoxic  $\text{NO}_2^-$  reductase activity and tissue XOR activity ( $r = 0.892$ ,  $p = 0.042$ ). The correlation between hypoxic  $\text{NO}_2^-$  reductase activity and mitochondrial inner surface area (D) is more striking, except for kidney ( $r = 0.9998$ ,  $p = 0.0001$ ).

metabolite formation in a tissue- and product-selective manner (Fig. 2, B–D). Tissue nitroso/nitrosyl products originated from  $\text{NO}_2^-$ , since their levels under identical hypoxic conditions were far less (<0.1%) without the supplied  $\text{NO}_2^-$  (23). Although each tissue examined was capable of hypoxia-induced,  $\text{NO}_2^-$ -dependent NO metabolite formation, it was most pronounced in liver, heart, and the RBC. The tissue-specificity of these responses to systemic hypoxia accords with previous demonstrations that endogenous substrates and the turnover of NO-related oxidative and nitrosative metabolites vary greatly among tissues (23, 26). Although there is limited NO production from  $\text{NO}_2^-$  by hypoxic RBC *in vitro* (Fig. 1), RBC exhibited the greatest relative RSNO formation during acute hypoxia *in vivo*. This finding is consistent with the S-nitrosation and nitrosylation of hemoglobin (Hb) by  $\text{NO}_2^-$  to form both, SNO-Hb and Hb-NO *in vitro* and *in vivo* (10); indeed, SNO-Hb is probably generated from circulating  $\text{NO}_2^-$  without the intermediate liberation of NO within the RBC (27).

**Kinetics and Concentration-dependence of  $\text{NO}_2^-$  Reduction to NO**—Liver effectively generates NO from  $\text{NO}_2^-$  (Fig. 1), has a multiplicity of potential reductases that can be pharmacologically investigated, and is readily available and easily perfused free of blood. Accordingly, liver was used to characterize more comprehensively the kinetics and chemistry of NO production from  $\text{NO}_2^-$  in tissue. The  $\text{NO}_2^-$  reductase activity of anoxic whole liver homogenate was linearly dependent upon the con-

centration of supplied  $\text{NO}_2^-$  (25–1000  $\mu\text{M}$ ) and, to a lesser extent, the amount of tissue protein employed (Fig. 3A). Because the generation of NO was measured over 4 min in each case and therefore represents the initial rate of NO formation, this observation suggests that whole liver homogenate grossly conforms to first order kinetics with respect to  $\text{NO}_2^-$  and, to a lesser extent, tissue protein concentration. In contrast to the results obtained with whole liver homogenate, no strict linearity was evident in the cytosolic fraction (S3) between NO formation and  $\text{NO}_2^-$  concentration, although the dependence upon protein concentration was similar to that in whole liver homogenate (Fig. 3B).

**$\text{NO}_2^-$  Reduction to NO Requires Enzymatic Activity**—To probe the involvement of enzymatic processes in hypoxic NO formation, aliquots of liver homogenate were subjected to heat pretreatment. Exposure of liver homogenate for 60 min to 56 or 80 °C inhibited  $\text{NO}_2^-$  reductase activity by 72 and >90%, respectively, relative to control, unheated tissue samples. These results are consistent with the conclusion that

thermolabile enzymes mediate the majority of hypoxic  $\text{NO}_2^-$  reduction to NO, either directly or indirectly (e.g. by modulating reducing equivalent supply).

**Putative Cellular  $\text{NO}_2^-$  Reductases**—To gain insight into potential mechanisms of tissue  $\text{NO}_2^-$  reduction,  $\text{NO}_2^-$ -dependent NO production was quantified as a function of reported literature values for tissue XOR activity (28) (Fig. 3C) and/or maximal oxidative phosphorylative capacity, indexed by Hulbert and Else (29) as inner mitochondrial membrane surface area (Fig. 3D). All tissues except kidney evidenced a strong linear relationship between tissue  $\text{NO}_2^-$  reductase activity as a function of mitochondrial membrane surface area (Fig. 3D). Because cytochrome oxidase activity directly correlates with inner mitochondrial membrane surface area (29), a linear relationship also exists between hypoxic tissue  $\text{NO}_2^-$  reduction to NO and cytochrome oxidase activity. Rat kidney (especially, renal medulla) deviates substantially from other organs in its greater dependence upon glycolysis *versus* oxidative phosphorylation for ATP production (30). Kidney  $\text{NO}_2^-$  reductive capacity may be limited to prevent NO-mediated mitochondrial inhibition due to the relatively high local  $\text{NO}_2^-$  concentrations that arise during renal anion filtration/secretion. The relatively weak relationship in the kidney between  $\text{NO}_2^-$  reductase activity and maximal oxidative metabolic capacity (Fig. 3D) supports the overall concept of a robust interrelationship between oxidative intermediary metabolism and  $\text{NO}_2^-$ -de-

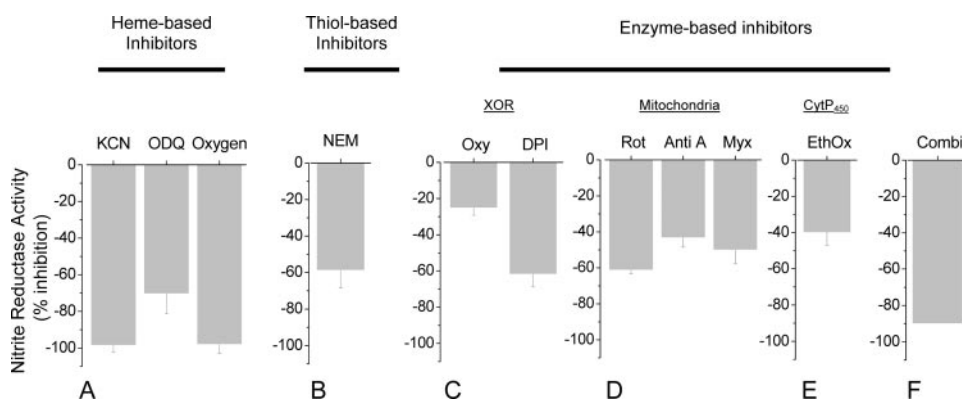


FIGURE 4. **Chemical sensitivity of hypoxic  $\text{NO}_2^-$  reduction to NO.** Exposure of whole liver homogenate to a variety of inhibitors targeting various cellular components (see supplementary Table S1 for details) shows that hypoxic  $\text{NO}_2^-$  reduction to NO is carried out by multiple enzymatic routes. Inhibitors for XOR, mitochondrial respiration, hemes, and thiols all attenuate hypoxic  $\text{NO}_2^-$  to NO conversion to varying degrees, with virtually complete inhibition by KCN and oxygen implicating metalloproteins as being most critical to the process ( $n = 3$ ). (Oxygen: 21%, medical-grade air; Oxy: oxypurinol; EthOx: ethoxyresorufin; Rot: rotenone; Anti A: antimycin A; Myx: myxothiazole; Combi: inhibitor mixture containing DPI, ethoxyresorufin, and rotenone).

pendent NO formation. Mitochondrial inner surface area, cytochrome oxidase, and/or oxygen utilization capacity reflect quantifiable, correlative parameters of this interrelationship.

**Chemical Sensitivity of  $\text{NO}_2^-$ -dependent NO Formation in Vitro**—To evaluate further the enzyme systems that may contribute to the formation of NO from  $\text{NO}_2^-$  in hypoxic liver, tissue samples were probed with an extensive array of inhibitors to target discrete enzymatic activities (supplemental Table S1). Cyanide and oxygen were among the most effective inhibitors, eliciting a concentration-dependent reduction of maximal NO formation from  $\text{NO}_2^-$  that reached >95% (Fig. 4A), suggesting the crucial involvement of metalloproteins and an oxygen-sensitive component. The heme-oxidant oxadiazolo[4,3-a]quinoxalin-1-one (ODQ) is also a potent inhibitor (70% at 10 mM) (Fig. 4A), suggesting the involvement of reduced hemes. Similar inhibition by the thiol alkylator *N*-ethylmaleimide (NEM) (~60% at 10 mM) (Fig. 4B) implies a role for free thiols in liver  $\text{NO}_2^-$  reductase activity under hypoxia. The xanthine oxidoreductase (XOR) inhibitor, oxypurinol (Oxy), partially (by 25%) inhibited hypoxic  $\text{NO}_2^-$  reduction, whereas preincubation of liver homogenate with the flavin inhibitor, diphenyleneiodonium (DPI), inhibited by as much as 62% (Fig. 4C), in further support of a role for XOR and/or mitochondrial aldehyde dehydrogenase (ALDH2). The inhibitory effects of cyanide and DPI are also consistent with an involvement of mitochondrial respiratory complexes in  $\text{NO}_2^-$  reduction. Other inhibitors of mitochondrial respiration (*i.e.* rotenone (Rot), antimycin A (Anti A), and myxothiazole (Myx)) also attenuated hypoxic NO formation from  $\text{NO}_2^-$  (Fig. 4D). Suppression of NO formation by ethoxyresorufin (EthOx) (Fig. 4E) implicates yet another mitochondrial and/or microsomal route of hypoxic  $\text{NO}_2^-$  reduction: EthOx selectively inhibits the cytochrome  $\text{P}_{450}$  CYP1A1, which is found in mitochondria and endoplasmic reticulum. The nonselective cytochrome  $\text{P}_{450}$  monooxygenase inhibitor proadifen was without effect. The aggregate inhibitor data allow conclusion that  $\text{NO}_2^-$  conversion to NO by hypoxic liver tissue is a multifactorial, metalloprotein- and thiol-dependent process, which is highly susceptible to inhibition by oxygen and involves XOR, several mitochondrial respiratory

chain complexes, and cytochrome  $\text{P}_{450}$ . In further support of the cooperative nature of this process, the combination of the three inhibitors rotenone, EthOx, and DPI (Combi) inhibited hypoxic  $\text{NO}_2^-$  reduction to NO to an extent greater than the inhibition elicited by each agent alone (Fig. 4F).

To investigate whether tissue  $\text{NO}_2^-$  reductase activity is sensitive to tissue oxidation state, ferricyanide (5 mM) was introduced prior to or after  $\text{NO}_2^-$  addition. Ferricyanide treatment pre-oxidizes potential reductases (*e.g.* ferrous hemoproteins) to diminish their reductase activity; ferricyanide exposure following  $\text{NO}_2^-$  addition promotes the

release of NO equivalents bound to ferrous hemoproteins. As reported by Shiva *et al.* (20) for heart homogenate, ferricyanide treatment significantly alters hepatic  $\text{NO}_2^-$  reductase activity (see supplemental information), implicating the involvement of redox-sensitive heme complexes. However, the enhanced reductase activity in the oxidized state seems to contradict any simple conception of a ferrous heme-based  $\text{NO}_2^-$  reductase. Addition of ferricyanide after incubation with  $\text{NO}_2^-$  under hypoxic (but not aerobic) conditions leads to large bursts of NO formation by liver homogenates. The sudden rise and exponential decay of the chemiluminescence signal is consistent with a reaction of ferricyanide with ferrous heme nitrosyl complexes (31). A comparison of the experimental data with mathematical models (see supplemental information) simulating NO generation from  $\text{NO}_2^-$  reduction and trapping by hemes predicts that the majority of nitrosyl products formed from  $\text{NO}_2^-$  must be derived without the intermediacy of free NO.

**Multiple Intracellular Compartments Contribute to Hypoxic NO Production from  $\text{NO}_2^-$** —To complement the inhibitor studies performed in whole liver homogenate and gain insight into the subcellular sites of hypoxic  $\text{NO}_2^-$  reductase activity in this organ, blood-free hepatic tissue was fractionated into mitochondrial, cytosolic, and microsomal fractions by standard differential centrifugation. The ability of each individual subfraction to form NO when supplied with 200  $\mu\text{M}$   $\text{NaNO}_2$  was examined during a 4-min incubation at 37 °C with nitrogen. Hepatic  $\text{NO}_2^-$  reductase activity under hypoxia was distributed selectively among the three major liver subfractions studied, with microsomes accounting for over half (~63%) of the total activity (Fig. 5A) when adjusted for compartmental fractional yield. Cytosolic NO formation from  $\text{NO}_2^-$  during hypoxia was sensitive to 100  $\mu\text{M}$  oxypurinol (52% inhibition), suggesting the involvement of XOR (and possibly other soluble proteins). Interestingly, subcellular fractions produced more NO than whole liver homogenate (Fig. 5B), implying that, when liver subfractions are combined, some consume NO and/or inhibit NO production by others. Consistent with the inhibitor studies, hypoxic conversion of  $\text{NO}_2^-$  to NO by liver mitochondria was stimulated ( $110 \pm 31\%$ ) by 100  $\mu\text{M}$  NADH (and >70% by 100

## Nitrite Processing by Hypoxic Tissues

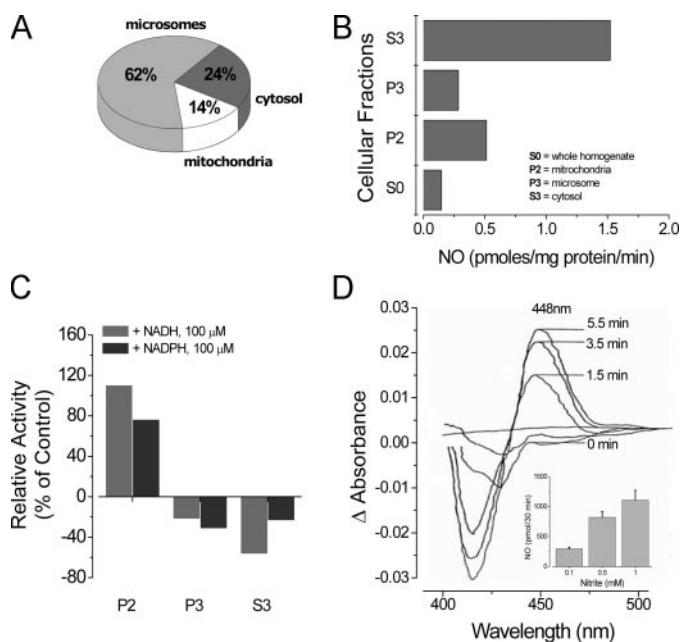


**FIGURE 5. Relative subcellular distribution and activity of hypoxic  $\text{NO}_2^-$  reduction to NO within liver tissue.** *A*, subcellular fractionation of hepatic tissue reveals that  $\text{NO}_2^-$ -dependent NO formation is nonuniformly distributed among cell compartments. *B*, specific activity of  $\text{NO}_2^-$  reduction to NO within subcellular fractions reveals that both cytosolic (S3) and mitochondrial (P2) compartments exhibit the highest specific  $\text{NO}_2^-$  reductase activities. *C*, pyridine nucleotide (NAD(P)H, 100  $\mu\text{M}$ ) enhances hypoxia-induced  $\text{NO}_2^-$  reduction to NO (70–110% increase from control) within the mitochondrial fraction ( $n = 2$ ). *D*, upon supplying  $\text{NO}_2^-$  to microsomal fractions (containing cyt  $\text{P}_{450}$ ), rapid formation of an iron-nitrite complex precedes formation of an iron-nitrosyl ( $\lambda_{\text{max}} = 448 \text{ nm}$ ) prior to release of NO. *Inset*, microsomal NO generation from  $\text{NO}_2^-$  is concentration-dependent. Increasing  $\text{NO}_2^-$  (0.1–1.0 mM) in hepatic microsomes potentiates NO formation ( $n = 3$ ).

$\mu\text{M}$  NADPH) (Fig. 5C), the electron source for the mitochondrial respiratory chain, which can increase the reduction potential of the system. The reason for the inhibition of  $\text{NO}_2^-$  reduction in cytosol and microsomes by NADPH is not obvious, but may reflect heightened consumption of NADPH by non-mitochondrial anabolic pathways (e.g. cytosolic fatty acid synthesis) stimulated by the added pyridine nucleotide. As a corollary to our observation that hepatic microsomes significantly contribute to nitrite reductase activity, spectral, and chemiluminescence studies confirm the sequence of microsomal nitrite binding, formation of a Cyt  $\text{P}_{450}$  iron-nitrosyl complex and NO release (supplemental information and Fig. 5D).

## DISCUSSION

The present study provides intriguing new insights into the oxygen-dependent processing of nitrite by mammalian tissues. The major findings are as follows: (a)  $\text{NO}_2^-$  is transported into cells rapidly irrespective of ambient oxygen tension. (b) While  $\text{NO}_2^-$  bioconversion to NO *in vitro* is limited under aerobic conditions, all tissues (especially the vasculature) readily convert  $\text{NO}_2^-$  to NO during hypoxia, and this is accompanied by nitrosation and nitrosylation of cell constituents. (c) This pattern of  $\text{NO}_2^-$  bioconversion to NO-related signaling products is recapitulated *in vivo*. (d) Although tissue  $\text{NO}_2^-$  reduction may be facilitated by non-enzymatic (e.g. disproportionation) and enzymatic mechanisms, tissue  $\text{NO}_2^-$  reductase activity is largely (>80%) heat labile, suggesting that enzymatic mechanisms pre-

dominate. (e) The kinetics of NO generation from  $\text{NO}_2^-$  appears to be first-order with respect to  $\text{NO}_2^-$  concentration, but do not obey simple first-order kinetics with respect to protein concentration. Hepatic and cardiac  $\text{NO}_2^-$ -dependent NO production under hypoxia commences after a delay and is sustained for a prolonged period of time. (f) Tissue  $\text{NO}_2^-$  reductase activity is associated with mitochondrial indices of oxidative phosphorylative capacity. (g) Inhibitor and subfractionation studies suggest that tissue  $\text{NO}_2^-$  conversion to NO is multifactorial, and  $\text{NO}_2^-$  reductase activity is distributed throughout different cell compartments. In liver, microsomal Cyt  $\text{P}_{450}$  moieties appear to be the dominant reductases, with significant contributions from mitochondria and cytosol (i.e. XOR). (h) Ferricyanide and modeling studies demonstrate that  $\text{NO}_2^-$  bioconversion under hypoxic conditions leads to the formation of nitrosyl products largely without the intermediacy of free NO.

The proposal that hypoxic vasodilation is a result of RBC-dependent  $\text{NO}_2^-$  conversion to NO (6, 10, 18, 19, 21, 22) proved to be a stimulus for investigating  $\text{NO}_2^-$  bioconversion. We (23) and others (15) have offered some initial characterization of  $\text{NO}_2^-$  metabolism in tissues. Increasing recognition of the biological significance of  $\text{NO}_2^-$  and its ubiquitous presence in mammalian systems (8) mandates further detailing of the elusive mechanisms through which  $\text{NO}_2^-$  is converted to NO and, perhaps, bioactive NO metabolites. Our present results and those of others (15) suggest that, at physiological  $\text{NO}_2^-$  levels, hypoxic RBC do not liberate significant amounts of NO. Instead, vascular tissue appears to have the greatest capacity to generate NO from  $\text{NO}_2^-$ . We now show that hypoxic  $\text{NO}_2^-$  reductase activity in tissues is accompanied by the nitrosation and nitrosylation of cellular targets, suggesting that some of the resulting NO metabolites may represent  $\text{NO}_2^-$ -related tissue effectors of (or markers for) hypoxic signaling.

Formation of NO from  $\text{NO}_2^-$  is an inefficient process on the order of 0.05 nmol/h/g wet tissue/ $\mu\text{M}$   $\text{NO}_2^-$  in liver and heart, with most of the reductase activity being thermolabile (i.e. enzymatic) (15). Accordingly, in tissues such as liver and heart with  $\text{NO}_2^-$  at a steady-state concentration of  $\sim 500 \text{ nM}$  (8, 23, 24), the expected NO production rate would be 0.025  $\mu\text{mol/kg/h}$ . The average rate of whole body NO production in rats and humans is significantly greater,  $\sim 1 \mu\text{mol/kg/h}$  (32). Tissues with higher  $\text{NO}_2^-$  concentrations such as aorta ( $\sim 20 \mu\text{M}$   $\text{NO}_2^-$ ) and with rates of  $\text{NO}_2^-$  conversion to NO at least twice that of the heart or liver, the NO production under hypoxic conditions could reach  $\sim 2 \mu\text{mol/kg/h}$ . It is thus conceivable that intrinsic NO generation from  $\text{NO}_2^-$  may have significant physiological importance in vascular tissue as an autonomous mediator of hypoxic vasodilation (11, 16). Conversely, one might question how the modest rates of  $\text{NO}_2^-$ -dependent NO production in heart and liver could account for the protective effects of  $\text{NO}_2^-$  against ischemia-reperfusion injury in these organs. Relevant insight may be obtained from our ferricyanide experiment, where the amount of free NO trapped by hemes accounts for only a small percentage of  $\text{NO}_2^-$ -derived NO. This result suggests that the production of free NO from  $\text{NO}_2^-$  under hypoxia may represent a relatively minor component of a potent chemical pathway that generates bioactive (i.e. tissue-protective) NO metabolites directly from  $\text{NO}_2^-$ .



Given the well-recognized interplay among oxygen, NO, and the mitochondrial electron transport chain (ETC) at the interface between tissue oxygen consumption and oxygen-dependent energy conservation, the mitochondrion is well-positioned to act as a "metabolic coordinator" (2, 33). Our observation that rates of  $\text{NO}_2^-$  conversion to NO correlate robustly with maximal mitochondrial respiratory capacity accords with the hypothesis that tissue oxygen demand and ambient oxygen concentration are operationally related through  $\text{NO}_2^-$ -dependent NO formation by, or more provocatively *for*, the ETC (12, 34, 35). This link between  $\text{NO}_2^-$ -dependent NO formation and oxidative intermediary metabolism is further underlined by the notable exception of renal tissue, the renal medulla relying largely on anaerobic metabolism (30). While these observations underscore the significance of mitochondria in  $\text{NO}_2^-$  bioconversion, the profile of  $\text{NO}_2^-$  reductases differs among tissues, and the mitochondrial compartment does not account for the majority of  $\text{NO}_2^-$  bioconversion. Far greater subcellular complexity is observed. At least in the liver, our combined inhibitor and cell-fractionation studies suggest that hepatic  $\text{NO}_2^-$  reductase activity occurs in the cytosol, the mitochondrion (along the ETC), and, predominantly, the microsomes (Cyt P<sub>450</sub>), with thiols and metalloproteins playing a crucial cooperative role. Microsomal heme-containing cytochromes are effective  $\text{NO}_2^-$  reductases (36, 37), as confirmed by the spectral studies herein.

Except for oxygen and cyanide, no one agent tested completely inhibited hypoxic  $\text{NO}_2^-$  reduction. However, a combination of three enzyme inhibitors (rotenone, EthOx, and DPI) virtually blocked all  $\text{NO}_2^-$ -dependent NO formation by liver homogenates. These observations are not easily reconciled with those of Li *et al.* (15), who failed to demonstrate any effect of rotenone on  $\text{NO}_2^-$  reductase activity and identified XOR and ALDH2 as important components of the cardiac and hepatic  $\text{NO}_2^-$  reductase system. Inhibitor nonspecificity undoubtedly accounts for some of these differences: although raloxifene has been used as an ALDH2 inhibitor (37), it also has potent effects on some microsomal Cyt P<sub>450</sub> species (*e.g.* 3A4) (38). Similarly, DPI is promiscuous and inhibits a variety of enzymes exhibiting flavin-dependent electron transfer including XOR, ALDH2, and other oxidoreductases. This demonstrates the weakness of isolated inhibitor studies and in part explains why our own inhibitor studies do not entirely accord with cell fractionation studies. For example, although rotenone inhibited 60% of the  $\text{NO}_2^-$  bioconversion in total liver homogenate, cell fractionation studies suggest that mitochondria contribute relatively modestly (14%) to overall hepatic  $\text{NO}_2^-$  reductase activity. We reconcile these observations by recognizing the limitations of inhibitor pharmacology, the nature of cell fractionation as a methodology that artificially divides a physiologically integrated, heuristic  $\text{NO}_2^-$  reductase, thereby preventing cooperative effects, and the potential for the inhibitor itself to enter into subfraction-selective reactions. Nonetheless, the inhibitor data do indicate that hepatic " $\text{NO}_2^-$  reductase" represents a biochemically and spatially complex activity that involves heme, iron-sulfur cluster, and molybdenum enzymes distributed among a number of organelles that cooperate to reduce  $\text{NO}_2^-$  to NO.

While there is compelling evidence herein and elsewhere that Hb is unlikely to contribute significantly to  $\text{NO}_2^-$ -depend-

ent NO formation in hypoxia due to the voracious capacity of deoxy/oxyHb to scavenge free NO, the significance of heme proteins as intracellular  $\text{NO}_2^-$  reductases remains unknown. To address this issue, we combined the use of ferricyanide (which putatively oxidizes iron from ferrous to ferric hemes) with modeling to dissect the role of hemes in hepatic and cardiac  $\text{NO}_2^-$  reductase activity. Our data suggest that: (a) Ferrous heme moieties within cells contribute substantially to NO scavenging. (b) Much of the NO liberated by ferricyanide is likely to have originated from nitrosyl groups generated directly from  $\text{NO}_2^-$ -dependent nitrosylation. (c) The enhanced effect on NO formation by ferricyanide pretreatment reflects either the limited participation of ferrous heme in  $\text{NO}_2^-$  bioconversion or, more likely, a mixed scavenging and liberating role for ferrous heme. Both the concentrations and reactivities of the different heme and other reductase moieties (microsomal, mitochondrial and cytosolic) will determine the net response to exogenous ferricyanide. NO liberation from microsomal ferrous cyt-P<sub>450</sub> nitrosyls is well-known (36) and may be counterbalanced by scavenging from other ferrous heme nitrosyl complexes slower in releasing NO and the influence of other reductases (*e.g.* XOR/ALDH2) (15). Pretreatment with ferricyanide may alter this balance (possibly across compartments) and favor early NO liberation. In other tissues (*e.g.* vasculature) where the heme profile and ratio of  $\text{NO}_2^-$  to heme proteins (and the activity of ferri-heme reductases) differ, the impact of scavenging may be attenuated, and NO release from heme moieties more profound. Indeed, recent experimental evidence points to a role for heme moieties in vascular  $\text{NO}_2^-$  bioconversion (16).

Hypoxic  $\text{NO}_2^-$  bioconversion to NO is effected with tissue-selectivity by an involved interplay of heme, iron-sulfur cluster, and molybdenum-containing enzymes, the nature and ratio of heme-dependent proteins (and other enzymes),  $\text{NO}_2^-$  and oxygen concentration, and redox state varying with tissue, time, and ambient conditions. The intricacy of these interactions and the redundancy exhibited by different  $\text{NO}_2^-$  reducing enzymes in different cell compartments within tissues raise important questions regarding the biological role of reductive  $\text{NO}_2^-$  metabolism to NO. Oxygen-dependent conversion of  $\text{NO}_2^-$  to NO renders it more suitable for hypoxic vasodilation (11) than L-arginine-driven, NO synthase-mediated hypoxic vasodilation, since the latter requires oxygen as a co-substrate to produce NO. However, the identification of redundant  $\text{NO}_2^-$  reductase activities in diverse tissues with varying functions and the association of this  $\text{NO}_2^-$  bioconversion with tissue oxidative phosphorylation capacity suggest that the biology of  $\text{NO}_2^-$  extends well beyond vasodilation and tissue protection. Based on the evidence presented herein, it is tempting to speculate that conversion of  $\text{NO}_2^-$  to NO is part of a conserved regulatory mechanism that acutely matches oxygen homeostasis to intermediary metabolism (37). As well acting directly on mitochondria (12, 35), the resulting nitrosation of master transcription factors such as HIF-1 $\alpha$  may have a profound impact on the cellular metabolic milieu (39). Different tissue compartments might affect their oxygen-sensing through the common path of  $\text{NO}_2^-$  conversion to NO. The resulting NO then acts to modify mitochondrial function and the cellular metabolic and transcriptional milieu. This hypothetical paradigm represents a

tuning mechanism through which eukaryotic cells might optimize their use of oxygen and carbon units for maximally efficient energy provision (2, 33, 35). Whether  $\text{NO}_2^-$  is indeed involved in such processes and whether there are differences in bioactivity between endogenous and exogenous  $\text{NO}_2^-$  will require further investigation.

### REFERENCES

- Schmidt, H. H., and Walter, U. (1994) *Cell* **78**, 919–925
- Erusalimsky, J. D., and Moncada, S. (2007) *Arterioscler. Thromb. Vasc. Biol.* **27**, 2524–2531
- Lancaster, J. R., Jr., and Xie, K. (2006) *Cancer Res.* **66**, 6459–6462
- Li, C. Q., and Wogan, G. N. (2005) *Cancer Lett.* **226**, 1–15
- Edmunds, N. J., Moncada, S., and Marshall, J. M. (2003) *J. Physiol.* **546**, 521–527
- Lundberg, J. O., Weitzberg, E., and Gladwin, M. T. (2008) *Nat. Rev. Drug Discov.* **7**, 156–167
- Stamler, J. S., Lamas, S., and Fang, F. C. (2001) *Cell* **106**, 675–683
- Bryan, N. S., Fernandez, B. O., Bauer, S. M., Garcia-Saura, M. F., Milsom, A. B., Rassaf, T., Maloney, R. E., Bharti, A., Rodriguez, J., and Feelisch, M. (2005) *Nat. Chem. Biol.* **1**, 290–297
- Mazzone, M., and Carmeliet, P. (2008) *Nature* **453**, 1194–1195
- Cosby, K., Partovi, K. S., Crawford, J. H., Patel, R. P., Reiter, C. D., Martyr, S., Yang, B. K., Waclawiw, M. A., Zalos, G., Xu, X., Huang, K. T., Shields, H., Kim-Shapiro, D. B., Schechter, A. N., Cannon, R. O., III, and Gladwin, M. T. (2003) *Nat. Med.* **9**, 1498–1505
- Maher, A. R., Milsom, A. B., Gunaruwan, P., Abozguia, K., Ahmed, I., Weaver, R. A., Thomas, P., Ashrafian, H., Born, G. V., James, P. E., and Frenneaux, M. P. (2008) *Circulation* **117**, 670–677
- Shiva, S., Sack, M. N., Greer, J. J., Duranski, M., Ringwood, L. A., Burwell, L., Wang, X., MacArthur, P. H., Shoja, A., Raghavachari, N., Calvert, J. W., Brookes, P. S., Lefer, D. J., and Gladwin, M. T. (2007) *J. Exp. Med.* **204**, 2089–2102
- Gonzalez, F. M., Shiva, S., Vincent, P. S., Ringwood, L. A., Hsu, L. Y., Hon, Y. Y., Aletras, A. H., Cannon, R. O., III, Gladwin, M. T., and Arai, A. E. (2008) *Circulation* **117**, 2986–2994
- Kumar, D., Branch, B. G., Pattillo, C. B., Hood, J., Thoma, S., Simpson, S., Illum, S., Arora, N., Chidlow, J. H., Jr., Langston, W., Teng, X., Lefer, D. J., Patel, R. P., and Kevil, C. G. (2008) *Proc. Natl. Acad. Sci. U. S. A.* **105**, 7540–7545
- Li, H., Cui, H., Kundu, T. K., Alzawahra, W., and Zweier, J. L. (2008) *J. Biol. Chem.* **283**, 17855–17863
- Alzawahra, W. F., Talukder, M. A., Liu, X., Samouilov, A., and Zweier, J. L. (2008) *Am. J. Physiol. Heart Circ. Physiol.*, **295**, H499–H508
- Basu, S., Grubina, R., Huang, J., Conradie, J., Huang, Z., Jeffers, A., Jiang, A., He, X., Azarov, I., Seibert, R., Mehta, A., Patel, R., King, S. B., Hogg, N., Ghosh, A., Gladwin, M. T., and Kim-Shapiro, D. B. (2007) *Nat. Chem. Biol.* **3**, 785–794
- Grubina, R., Huang, Z., Shiva, S., Joshi, M. S., Azarov, I., Basu, S., Ringwood, L. A., Jiang, A., Hogg, N., Kim-Shapiro, D. B., and Gladwin, M. T. (2007) *J. Biol. Chem.* **282**, 12916–12927
- Isbell, T. S., Gladwin, M. T., and Patel, R. P. (2007) *Am. J. Physiol. Heart Circ. Physiol.* **293**, H2565–H2572
- Shiva, S., Huang, Z., Grubina, R., Sun, J., Ringwood, L. A., MacArthur, P. H., Xu, X., Murphy, E., Darrley-USmar, V. M., and Gladwin, M. T. (2007) *Circ. Res.* **100**, 654–661
- Crawford, J. H., Isbell, T. S., Huang, Z., Shiva, S., Chacko, B. K., Schechter, A. N., rley-USmar, V. M., Kerby, J. D., Lang, J. D., Jr., Kraus, D., Ho, C., Gladwin, M. T., and Patel, R. P. (2006) *Blood* **107**, 566–574
- Huang, K. T., Keszler, A., Patel, N., Patel, R. P., Gladwin, M. T., Kim-Shapiro, D. B., and Hogg, N. (2005) *J. Biol. Chem.* **280**, 31126–31131
- Bryan, N. S., Rassaf, T., Maloney, R. E., Rodriguez, C. M., Saijo, F., Rodriguez, J. R., and Feelisch, M. (2004) *Proc. Natl. Acad. Sci. U. S. A.* **101**, 4308–4313
- Feelisch, M., Rassaf, T., Mnaimneh, S., Singh, N., Bryan, N. S., Jourd'Heuil, D., and Kelm, M. (2002) *FASEB J.* **16**, 1775–1785
- Rickwood, D. (1993) *Preparative Centrifugation: A Practical Approach*, Oxford University Press, New York
- Rodriguez, J., Maloney, R. E., Rassaf, T., Bryan, N. S., and Feelisch, M. (2003) *Proc. Natl. Acad. Sci. U. S. A.* **100**, 336–341
- Angelo, M., Singel, D. J., and Stamler, J. S. (2006) *Proc. Natl. Acad. Sci. U. S. A.* **103**, 8366–8371
- Parks, D. A., and Granger, D. N. (1986) *Acta Physiol. Scand. Suppl* **548**, 87–99
- Hulbert, A. J., and Else, P. L. (1989) *Am. J. Physiol.* **256**, R63–R69
- Cohen, J. J. (1979) *Am. J. Physiol.* **236**, F423–F433
- Gladwin, M. T., Wang, X., Reiter, C. D., Yang, B. K., Vivas, E. X., Bonaventura, C., and Schechter, A. N. (2002) *J. Biol. Chem.* **277**, 27818–27828
- Castillo, L., Beaumier, L., Ajami, A. M., and Young, V. R. (1996) *Proc. Natl. Acad. Sci. U. S. A.* **93**, 11460–11465
- Moncada, S., and Erusalimsky, J. D. (2002) *Nat. Rev. Mol. Cell Biol.* **3**, 214–220
- Kozlov, A. V., Staniek, K., and Nohl, H. (1999) *FEBS Lett.* **454**, 127–130
- Benamar, A., Rolletschek, H., Borisjuk, L., Velange-Macherel, M. H., Curién, G., Mostefai, H. A., Andriantsitohaina, R., and Macherel, D. (2008) *Biochim. Biophys. Acta*, **1777**, 1268–1275
- Kozlov, A. V., Dietrich, B., and Nohl, H. (2003) *Br. J. Pharmacol.* **139**, 989–997
- Li, H., Liu, X., Cui, H., Chen, Y. R., Cardounel, A. J., and Zweier, J. L. (2006) *J. Biol. Chem.* **281**, 12546–12554
- Zhou, S., Yung, C. S., Cher, G. B., Chan, E., Duan, W., Huang, M., and McLeod, H. L. (2005) *Clin. Pharmacokinet.* **44**, 279–304
- Kaelin, W. G., Jr., and Ratcliffe, P. J. (2008) *Mol. Cell* **30**, 393–402